Desalination 614 (2025) 119218

Contents lists available at ScienceDirect

Desalination

journal homepage: www.elsevier.com/locate/desal

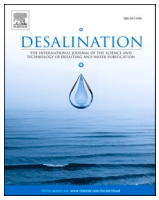

Deep eutectic solvent flow electrodes for high-voltage desalination via flow electrode capacitive deionisation

Elena Gabirondo [a,b,c,1], Hafiz M. Saif [a,1], Vitor D. Alves [d], João G. Crespo [a,e], Liliana C. Tomé [a,c,*], Sylwin Pawlowski [a,**]

[a] LAQV-REQUIMTE, Department of Chemistry, NOVA School of Science and Technology, FCT NOVA, Universidade NOVA de Lisboa, 2829-516 Caparica, Portugal
[b] POLYMAT and Department of Polymers and Advanced Materials: Physics, Chemistry and Technology, Faculty of Chemistry, University of the Basque Country UPV/EHU, P° Manuel de Lardizabal, 3, 20018 Donostia-San Sebastian, Spain
[c] CEMMPRE, ARISE, Department of Chemical Engineering, University of Coimbra, Rua Sílvio Lima, 3030-790 Coimbra, Portugal
[d] LEAF—Linking Landscape, Environment, Agriculture and Food Research Center, Associate Laboratory TERRA, Instituto Superior de Agronomia, Universidade de Lisboa, Tapada da Ajuda, 1349-017 Lisboa, Portugal
[e] Instituto de Tecnologia Química e Biológica António Xavier, Universidade NOVA de Lisboa, Av. da República, 2780-157 Oeiras, Portugal

HIGHLIGHTS

- Deep eutectic solvents (DES) were used as flow electrode electrolytes.
- Water addition strengthens DES gel-like structure despite lowering its viscosity.
- The operation of FCDI with DES flow electrodes was stable for up to 2.2 V.
- Desalination efficiency and rate are higher when DES flow electrodes are used.
- No DES traces were detected in desalinated water, confirming its safety.

GRAPHICAL ABSTRACT

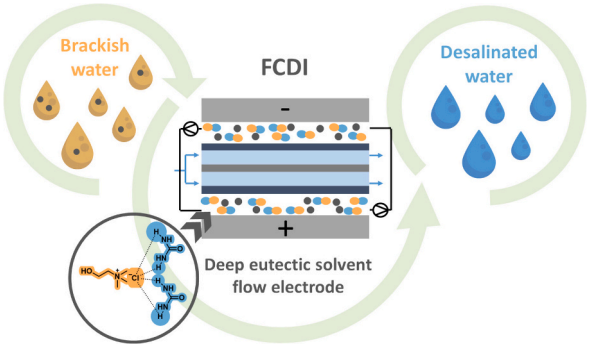

ARTICLE INFO

Keywords:
Flow electrode capacitive deionisation
Desalination
Deep eutectic solvents
Flow electrodes

ABSTRACT

This study pioneers the application of deep eutectic solvents (DES) as electrolytes in flow electrode capacitive deionisation (FCDI) desalination systems, providing a novel and improved alternative to aqueous flow electrodes. The deep eutectic solvent, choline chloride-urea (ChCl-U), was selected for its wide electrochemical stability window, allowing voltages exceeding 1.23 V, which is the limit for aqueous flow electrodes. The effect of water doping on the viscosity and performance of the DES flow electrodes was also investigated. Cyclic voltammetry confirmed the electrochemical stability, while rheological and electrochemical impedance spectroscopy revealed that the addition of water reduced the viscosity and enhanced the conductivity of ChCl-U, making it suitable for use as an electrolyte in FCDI. Desalination experiments were performed within a potential range of up to 2.2 V.

* Correspondence to: L.C. Tomé, CEMMPRE, ARISE, Department of Chemical Engineering, University of Coimbra, Rua Sílvio Lima, 3030-790 Coimbra, Portugal.
** Correspondence to: S. Pawlowski, LAQV-REQUIMTE, Department of Chemistry, NOVA School of Science and Technology, FCT NOVA, Universidade NOVA de Lisboa, 2829-516 Caparica, Portugal.
E-mail addresses: liliana@eq.uc.pt (L.C. Tomé), s.pawlowski@fct.unl.pt (S. Pawlowski).
[1] Equally contributing authors.

https://doi.org/10.1016/j.desal.2025.119218
Received 6 June 2025; Received in revised form 14 July 2025; Accepted 17 July 2025
Available online 18 July 2025

The ChCl-U flow electrode, containing 20 wt% water and 10 wt% activated carbon, achieved the best balance between desalination efficiency (83 %), desalination rate (0.17 mg/cm^2.min), and effluent quality. Furthermore, ^{1}H NMR analysis confirmed the absence of traces of the deep eutectic solvent in the dilute stream. The results highlight the potential of DES flow electrodes to enhance desalination processes by enabling higher operational voltages and improved performance, thereby paving the way for more efficient FCDI desalination systems.

1. Introduction

Access to clean drinking water is crucial for daily life, agriculture, and other industrial activities. In recent decades, with an increasing global population, rising economic activity, and growing impact of climate change on the environment, the availability of clean drinking water has diminished [1,2]. Furthermore, the demand for freshwater exceeds the available supply, highlighting the need for alternative water sources such as brackish water, seawater, and wastewater [3].

Flow electrode capacitive deionisation (FCDI) is an emerging electromembrane desalination method in which flow electrodes are employed to extract ions from saline water through electrosorption [4–6]. FCDI provides several advantages over other desalination methods, such as capacitive deionisation (CDI) and reverse osmosis (RO). Unlike batch-mode CDI, FCDI allows for continuous desalination owing to the in-situ regeneration of the flow electrodes [4–8]. Electrode fouling, a common issue in CDI systems, is also reduced in FCDI due to the membranes separating the treated feed water from the flow electrodes [9,10]. Furthermore, FCDI operates under atmospheric pressure, which lowers the infrastructure and energy costs compared to high-pressure systems such as RO [11,12]. These advantages make FCDI an effective desalination process that presents a feasible opportunity for scale-up [13–15].

The flow electrodes (carbon slurries) used in FCDI consist of activated carbon particles dispersed in an electrolyte, which is typically an aqueous medium. Various electrode materials have been developed to enhance the capabilities of FCDI systems [12,16–18]. In particular, carbon nanotubes, graphene-based composites, silver nanoclusters (NCs) and carbon nanofiber aerogels have emerged as promising candidates because of their exceptional electrical conductivity and large surface area [19–24], demonstrating specific capacitance and ion adsorption capacities that are 1.5 to 2.5 times higher than those of traditional carbon-based electrodes. The incorporation of these advanced materials has resulted in FCDI systems with higher desalination rates, improved energy efficiencies, and longer operational lifetimes [25–27]. However, it is crucial that the applied potential remains below the standard electrode potential of water (1.23 V), at which point the water molecules begin to break into hydrogen and oxygen. Surpassing this voltage across the electric double layer triggers water electrolysis, which results in unwanted side reactions. Nevertheless, in practical applications, the total voltage applied across the FCDI cell may exceed 1.23 V to compensate for inherent system resistances, thereby preventing hydrolysis. The initiation of water splitting is influenced by local potential differences at the molecular level, which can vary depending on system design and operational conditions [28]. Additionally, water electrolysis not only consumes energy, but also damages system components, such as membranes and electrodes, due to pH changes. Moreover, maintaining the quality of the treated water at the desired levels is challenging because of the pH fluctuations that occur when the FCDI system operates at elevated voltages while using water as an electrolyte. Therefore, an electrochemically stable electrolyte at high voltages is essential to address this challenge.

Deep eutectic solvents (DES) are promising alternatives to conventional organic solvents and their predecessors, ionic liquids, for a myriad of applications, including electrochemistry [29–32]. The variety of starting materials and their possible combinations provides a versatile tool for controlling the physicochemical properties (such as viscosity, conductivity, and ion solvation ability) of the resulting DES. Additionally, many deep eutectic solvents offer remarkable advantages, including low cost of components and straightforward preparation (100 % atom economy). Altogether, these benefits have elevated DES to a prominent position in the quest for sustainable solvents, thereby creating new opportunities for the development of more efficient and economical processes. In particular, using DES as a flow electrode electrolyte can present several advantages in FCDI, as certain DES demonstrate broader electrochemical stability than water [33–35]. This could enable the application of voltages exceeding 1.23 V without causing electrolysis. The chosen deep eutectic solvent must be compatible with other FCDI components, such as ion-exchange membranes, and the composition of the DES flow electrode should be meticulously optimised to achieve an ideal balance between the conductivity, viscosity, and ion adsorption capacity.

To the best of our knowledge, this is the first study to introduce the use of a DES flow electrodes in FCDI applications. A eutectic mixture of choline chloride and urea (ChCl-U) was selected because of its electrochemical stability [36], low cost, and widespread availability. Cyclic voltammetry measurements were first conducted to investigate the electrochemical properties of the DES and determine its stable operating potential window. Electrochemical impedance spectroscopy (EIS) was employed to assess conductivity. The impact of doping DES with water, aiming to modulate its viscosity and, consequently, the FCDI desalination performance, was also explored. Finally, desalination experiments using the ChCl-U flow electrodes were carried out within a potential range of up to 2.2 V, and the results were benchmarked against the performance of traditional aqueous flow electrodes, highlighting the potential of DES to push the boundaries of FCDI desalination capacity.

2. Materials and methods

2.1. Materials

Choline chloride (ChCl) and urea (U) were purchased from Sigma-Aldrich and were used to prepare the deep eutectic solvent. Activated carbon (YP50F) (with a specific surface area of 1606 m^2/g, a specific capacitance of 9 F/g, a salt adsorption capacity of 122 mg/g and a mean particle diameter of 6.33 μm [37]), specifically designed for capacitors, was acquired from Chemviron (Germany) to prepare the flow electrodes. Model brackish water was prepared using NaCl salt obtained from Honeywell Fluka™ Chemicals (Germany). All solutions were prepared using Milli-Q water (Millipore).

2.2. Preparation of flow electrodes

Two types of flow electrodes were prepared, namely DES flow electrodes and aqueous flow electrodes. All the flow electrodes contained 10 wt% YP50F activated carbon (AC).

To prepare DES flow electrodes, choline chloride and urea were first mixed in a 1:2 molar ratio. The mixture was heated to 70 °C and stirred for 2 h to form the deep eutectic solvent. Following this, 10 wt% YP50F AC was added to the deep eutectic solvent and stirred for 24 h to achieve a uniform carbon dispersion. To adjust the viscosity of the DES flow electrodes, varying amounts of deionised water (10, 20, or 30 wt%) were doped into the mixture.

For the aqueous flow electrode, a 1 g/L NaCl solution was first prepared. Subsequently, 10 wt% YP50F AC was added. The mixture was stirred for 24 h to achieve homogeneous carbon dispersion.

2.3. ^1H nuclear magnetic resonance (^1H NMR)

To confirm the formation of the deep eutectic solvent and the absence of traces of the deep eutectic solvent in the dilute stream, ^1H Nuclear Magnetic Resonance spectroscopy was performed using an Avance DPX 300 NMR spectrometer (Bruker, Germany) operating at a resonance frequency of 300.16 MHz. Deuterated dimethyl sulfoxide (DMSO) was used as the solvent at room temperature. The experimental parameters were as follows: 10 mg of sample; 3 s acquisition time; 1 s delay time; 8.5 μs pulse; spectral width of 5000 Hz, and 32 scans.

2.4. Differential scanning calorimetry (DSC)

Differential scanning calorimetry (DSC) measurements of the DES flow electrodes were performed using a DSC8500 instrument (Perkin Elmer, Inc.) calibrated with indium and tin standards. Samples of around 3 mg were sealed in non-recyclable aluminium hermetic pans and analysed under a nitrogen atmosphere by heating and cooling cycles at 10 °C/min. Initially, the samples were heated from 25 °C to 100 °C and held at this temperature for 3 min to eliminate any thermal history. The samples were then cooled to −50 °C and maintained at this temperature for 10 min. To examine the phase transition behaviour, second-run heating cycles were performed and utilised for analysis.

2.5. Cyclic voltammetry

Cyclic voltammetry measurements of the DES flow electrodes were carried out using a Vertex 5A potentiostat (Ivium Technologies, The Netherlands). For each measurement, 3 cycles were performed at a scan rate of 5 mV/s, and the average values are reported.

2.6. Rheological tests

A controlled stress rheometer (Thermo Scientific, HAAKE MARS III, Germany) equipped with a Peltier heating system was utilised to assess the viscosity of the flow electrodes. The measurements were conducted using a coaxial cylinder geometry (Rotor CC25 DIN Ti) at a shear rate range of 0.1 to 200 s^{-1}, while maintaining a constant temperature of 30 °C.

The viscoelastic properties of the samples were assessed under tension within the viscoelastic region by performing a frequency sweep between 0.01 and 10 Hz. The storage (G′, Pa) and loss (G″, Pa) moduli were measured at a constant temperature of 30 °C.

2.7. Electrochemical impedance spectroscopy (EIS)

Electrochemical impedance spectroscopy (EIS) was conducted using a Vertex 5A potentiostat (Ivium Technologies, The Netherlands) to analyse the conductivity of the flow electrodes. The experiments were carried out over a frequency range of 20 kHz to 0.2 Hz with a sinusoidal perturbation of 10 mV amplitude. Each flow electrode had a volume of 200 mL and was passed through a conductivity cell (Fig. S1) at a flow rate of 100 mL/min.

The conductivity cell consisted of a polycarbonate tube with an inner diameter of 1.3 cm and length of 13 cm. To perform EIS on the flowing electrodes within the tube, four platinum wire components, each with a diameter of 1 mm, were placed inside the tube as shown in Fig. S1. Details of the construction of this conductivity cell are described elsewhere [38].

The electrical conductivity of the flow electrodes was calculated using Eq. (1):

$$\sigma = \frac{1}{R_{HF}} \frac{\delta}{A}, \tag{1}$$

where, R_{HF} is the real limit of the impedance at high frequency, and $\frac{\delta}{A}$ represents the cell constant determined to be 0.76 cm^{-1}.

2.8. Desalination test

Desalination tests were carried out using a single cycle with a separate concentrate chamber (SCSC) flow electrode capacitive deionisation (FCDI) cell (Fig. 1). Among several operational FCDI configurations, the SCSC configuration was selected because it allows the FCDI process to operate continuously without significant fluctuations in various parameters, such as the pH of the treated water [39]. The FCDI cell was constructed using an electrodialysis stack from MEGA (Czech Republic), which was modified for this purpose. The platinum-coated titanium electrodes were replaced with CNC-milled graphite plates (Fig. S2) with a serpentine channel comprising 36 segments, each 2 mm wide, 2 mm deep, and 34 mm long [40], served as current collectors and flow electrode channels. Fumasep® FAB-PK-130 anion-exchange membranes (AEMs) were installed in front of the electrode compartments, while a Fumasep® FKB-PK-130 cation-exchange membrane (CEM) separated the dilute and concentrate compartments. The thickness of the dilute and concentrate compartments was 1.6 mm, while the thickness of all ion-exchange membranes was 150 μm. The active contact area between the channel and the membrane was 26.58 cm^2.

Each desalination experiment lasted for 1 h, employing a constant voltage mode, using a Vertex 5A potentiostat (Ivium Technologies, The Netherlands). A conductivity/pH multimeter (Horiba Laqua-PC1100, Japan) was used to measure the conductivity and pH of the dilute and concentrated streams at 2-second intervals. The associated error with the conductivity measurements was ±0.5 %. The volume of flow electrodes was 200 mL in each experiment, and it was recirculated through the FCDI cell at a flow rate of 100 mL/min. The feed mimicking brackish water was an aqueous solution of 1.5 g/L NaCl. The feed solution was split equally between the concentrate and dilute compartments at a flow rate of 2.5 mL/min each. Continuous recirculation of the flow electrodes between the anode and cathode compartments enabled simultaneous desalination and electrode regeneration within the same system, allowing for efficient and continuous desalination. The schematic representation of the experimental setup is shown in Fig. S3.

The desalination efficiency was calculated using Eq. (2):

$$\textit{Desalination efficiency}\ (\%) = \frac{(C_{feed} - C_{dilute})}{C_{feed}} \times 100, \tag{2}$$

where C_{feed} is the feed NaCl concentration (mg/L) and C_{dilute} is the effluent NaCl concentration in the dilute stream (mg/L).

The salt removed $\Gamma(g)$ during the experiment was calculated using Eq. (3), and the desalination rate (mg/cm^2.min) was calculated using Eq. (4):

$$\Gamma = \int_0^t Q(C_{feed} - C_{dilute})dt, \tag{3}$$

$$\textit{Desalination rate} = \frac{\Gamma \times 1000}{A \times t}, \tag{4}$$

where Q is the volumetric flow rate (m^3/min), A is the effective contact area (cm^2) between the flow electrode and ion exchange membrane, and t is the duration of the experiment (min).

3. Results and discussion

3.1. Rheology and stability of DES and aqueous flow electrodes

The ChCl-U deep eutectic solvent (Fig. 2a) was prepared by mixing ChCl and urea at a 1:2 molar ratio. The resulting ChCl-U mixture was characterised by ^1H NMR spectroscopy. The proton signals of urea shifted to higher frequencies, confirming the formation of a deep eutectic solvent (Fig. 2b). Additionally, the thermal properties of the

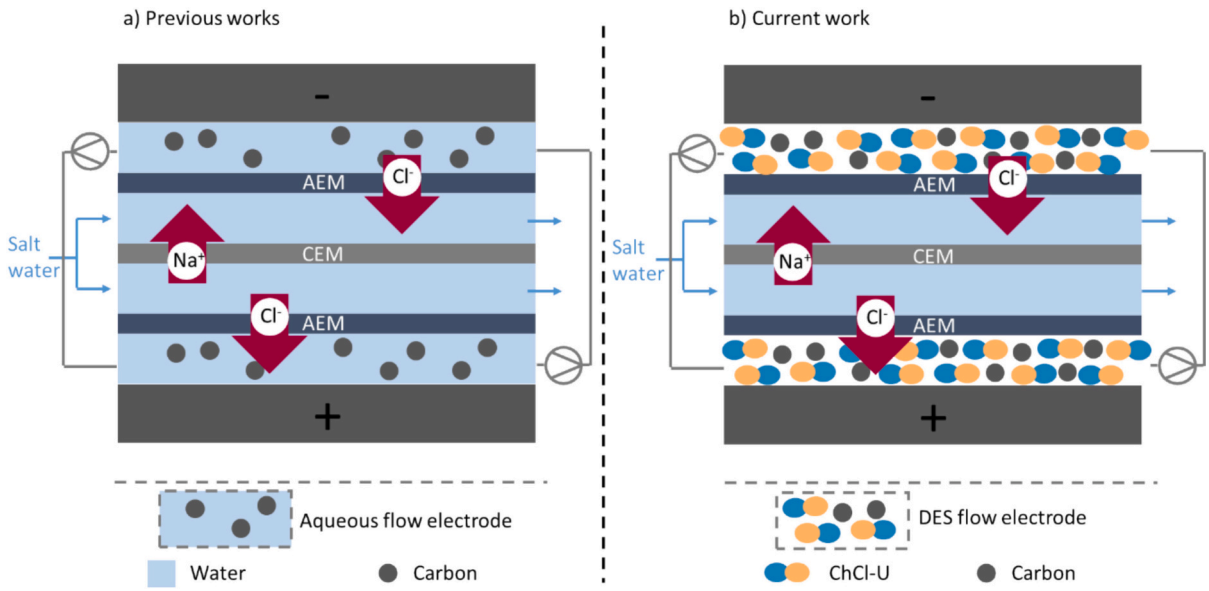

Fig. 1. Schematic representation of the FCDI setup for desalination tests with (a) aqueous flow electrode and (b) DES flow electrode.

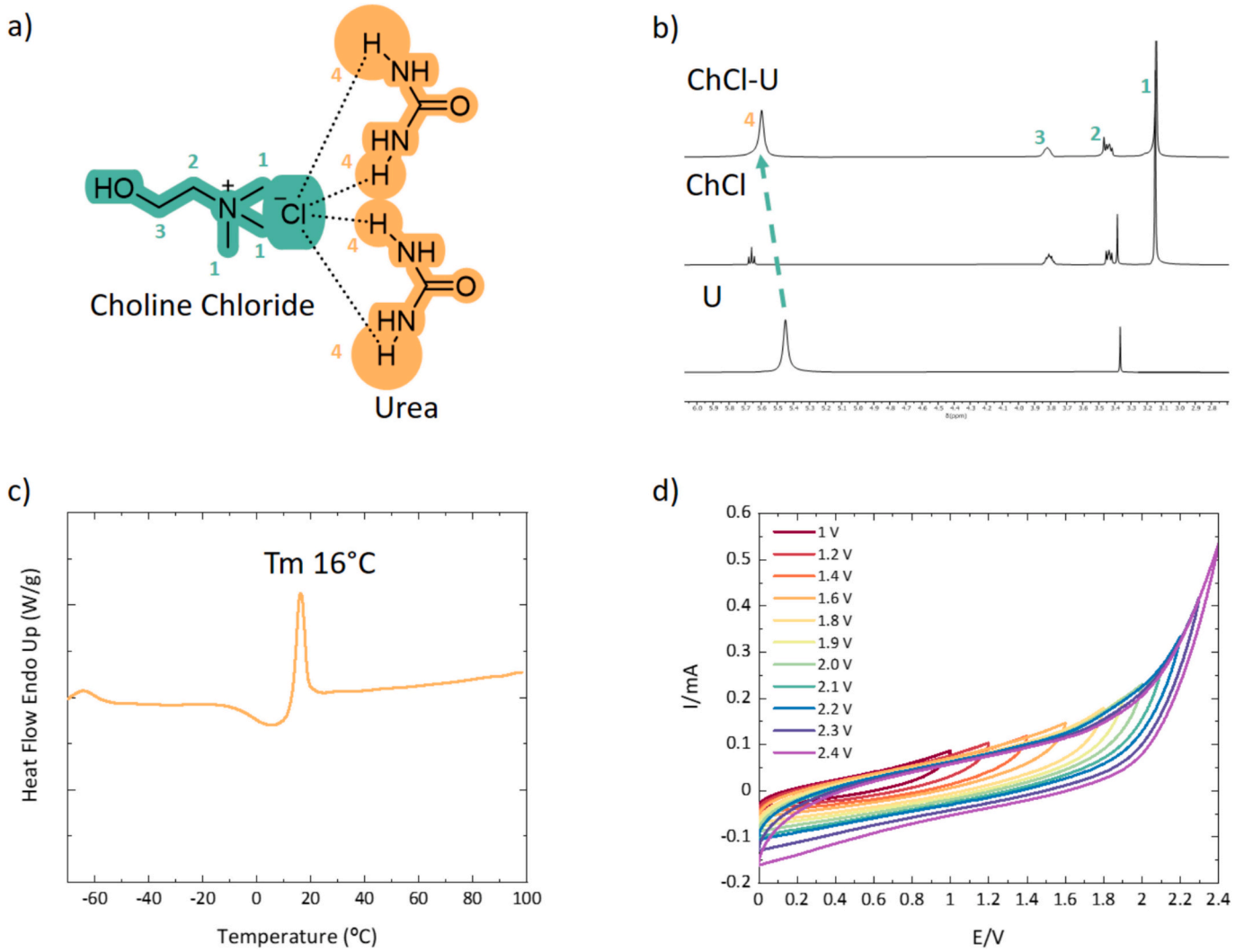

Fig. 2. (a) Chemical structure, (b) ^{1}H NMR spectra of choline chloride (ChCl), urea (U) and the resulting deep eutectic solvent (ChCl-U), (c) thermal properties, and (d) cyclic voltammetry of the deep eutectic solvent ChCl-U.

solvent were studied, and a melting temperature of 16 °C was determined by DSC (Fig. 2c), indicating a significant reduction compared to the melting temperatures of the starting compounds: choline chloride (302 °C) and urea (133 °C) [36]. Cyclic voltammetry (CV) was conducted to investigate the electrochemical behaviour of the deep eutectic solvent (Fig. 2d). The CV curves recorded at 5 mV/s showed no significant deviation from a quasi-rectangular shape up to 2.2 V, indicating a considerably broader potential window than that of water, which undergoes electrolysis at 1.23 V.

However, the viscosity of ChCl-U is considerably higher than that of water (Fig. 3a), rendering it unsuitable for direct use as an electrolyte in preparing a flow electrode for the FCDI system. It is worth noting that ChCl-U displayed Newtonian behaviour and maintained a constant viscosity of 0.6 Pa·s regardless of the shear rate. Under the same conditions, the viscosity of water was approximately 0.001 Pa·s, which is 600 times lower. Furthermore, the incorporation of activated carbon in flow electrodes to enhance ion adsorption capacity (to improve desalination efficiency) results in an increase in viscosity; in this instance, reaching 1.14 Pa·s at a shear rate of 200 s^{-1}, accompanied by an observable shear thinning behaviour (Fig. 3a).

To reduce the viscosity of the flow electrode and make it suitable for flow electrode applications in FCDI, various amounts of water (10, 20, and 30 wt%) were doped into the DES flow electrode (Fig. 3b). Introducing 10 wt% of water into the DES flow electrode reduced its viscosity to 0.09 Pa·s at a shear rate of 200 s^{-1}. Increasing the water content further resulted in even greater viscosity reductions, with values of 0.04 Pa·s and 0.02 Pa·s observed for water contents of 20 wt% and 30 wt%, respectively.

It is crucial to note that adding water to deep eutectic solvents can compromise their stability beyond a certain threshold of water content, as large amounts of water may lead to breakdown of the eutectic mixture [41,42]. Higher water content can also adversely affect the electrochemical characteristics by narrowing the potential window of the flow electrode. To investigate this phenomenon, cyclic voltammetry (CV) measurements were conducted using the DES flow electrodes, both with and without water (Fig. 4a-d).

The CV results indicate that adding water to the DES flow electrode enhances the recorded current values at higher applied potentials. At 2.2 V, the current increased from 1.58 mA to 2.50 mA with the addition of 10 wt% water. Further increments were observed for higher water contents, reaching 3.29 mA for 20 wt% water and 4.2 mA for 30 wt% water. Notably, the doping of water into the DES flow electrode did not compromise its stability up to 20 wt% H_2O. However, at 30 wt% H_2O, as evidenced by the CV (Fig. 4d) and DSC results (Fig. 9a), the eutectic nature was lost, and the system was no longer stable at 2.2 V.

Ionic resistance and conductivity measurements were conducted using DES flow electrodes and were compared with those of the aqueous flow electrodes (Table 1). The ChCl-U itself exhibited a conductivity of 0.59 mS/cm, which increases slightly to 0.88 mS/cm with the addition of 10 wt% AC, but remains lower than the conductivity of the 1 g/L NaCl aqueous solution with 10 wt% AC, which shows a conductivity value of 2.65 mS/cm. With the addition of 10 wt% water, the ionic resistance decreased by 94 %, resulting in a value of 51.8 Ohm and a conductivity of 14.68 mS/cm. Further addition of water reduced the ionic resistance even more, reaching 19.3 Ohm and a conductivity of 39.39 mS/cm when 30 wt% water was doped into the DES flow electrode. As expected, the addition of water to the system lowered the viscosity (Fig. 3b), rendering the solution less resistant to flow.

This change in viscosity facilitates ion movement within the mixture, thereby decreasing ionic resistance. This phenomenon is commonly observed for hydrophilic deep eutectic solvents. The increase in conductivity can be attributed to the ability of water to disrupt the hydrogen-bonding network of the DES, thereby enhancing the ion mobility. Water molecules act as additional solvent molecules, aiding the mobility of ionic species and facilitating better ionic conduction throughout the system. Consequently, the ionic conductivity of the system increased because the lower ionic resistance allowed the ions to move more freely.

3.2. Desalination tests with DES and aqueous flow electrodes

Fig. 5a presents the chronoamperometric curves obtained during desalination tests in the FCDI cell using various DES flow electrodes and 1 g/L NaCl aqueous flow electrode with 10 wt% AC for comparison.

When the flow electrode, composed of a 1 g/L NaCl solution and 10 wt% AC in water was utilised, a steady current of 82 mA and a dilute stream conductivity of 0.80 mS/cm were recorded at an applied potential of 1.2 V. Theoretically, it is inadvisable to increase the potential beyond this value due to the risk of water electrolysis. It is worth noting that the pH of the dilute stream, approximately 9, indicates that even this applied potential may have already been too high (Fig. 6). The observed increase in pH during electrochemical desalination can be attributed to oxygen reduction and/or hydrogen evolution. Specifically, water undergoes a Faradaic reaction where it is reduced to produce hydrogen gas and hydroxide ions. Consequently, the generated hydroxyl ions increased the pH. This effect becomes increasingly pronounced as the operational voltage is raised [43,44].

Conversely, the use of DES flow electrodes enabled the application of

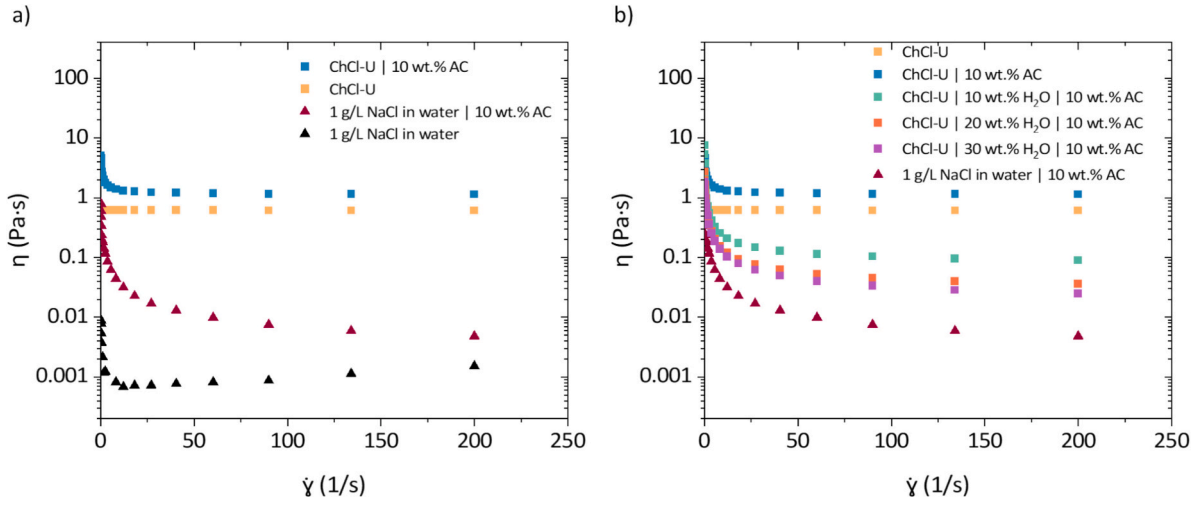

Fig. 3. Viscosity study of (a) 1 g/L NaCl in water and ChCl-U deep eutectic solvent, with and without 10 wt% of activated carbon (AC) and (b) ChCl-U deep eutectic solvent with 10 wt% activated carbon (AC) and varying water content.

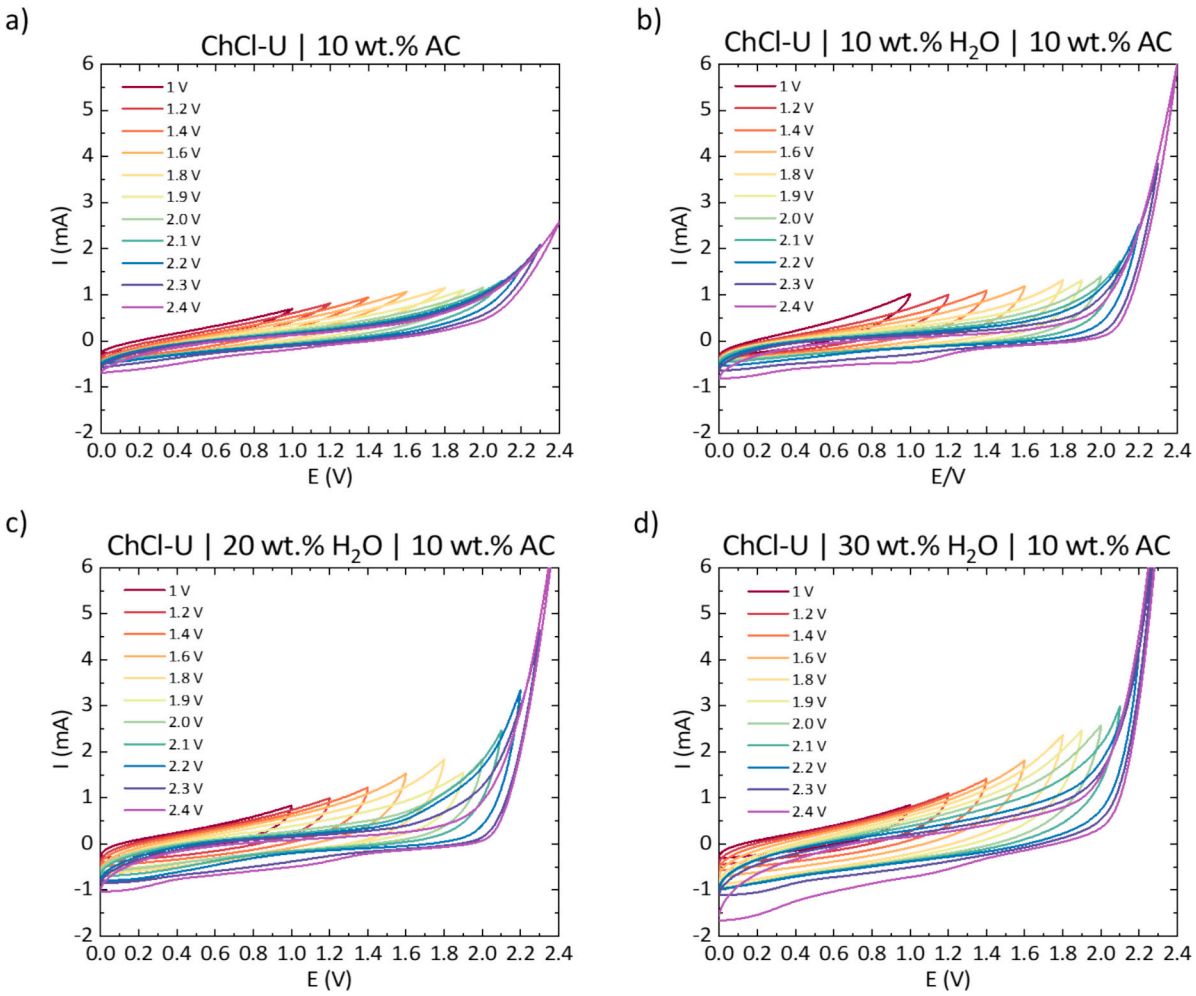

Fig. 4. Cyclic voltammetry results obtained for: (a) ChCl-U | 10 wt% activated carbon, (b) ChCl-U | 10 wt% H_2O | 10 wt% activated carbon, (c) ChCl-U | 20 wt% H_2O | 10 wt% activated carbon and (d) ChCl-U | 30 wt% H_2O | 10 wt% activated carbon.

Table 1
Ionic resistance and conductivity values for aqueous and DES flow electrodes containing different wt% of water and 10 wt% of activated carbon.

	Ionic resistance (Ohm)	Conductivity (mS/cm)
Water | 10 wt% AC	101,707.0	7.47×10^{-3}
ChCl-U	1289.0	0.59
ChCl-U | 10 wt% AC	859.5	0.88
1 g/L NaCl | 10 wt% AC	286.5	2.65
ChCl-U | 10 wt% H_2O | 10 wt% AC	51.8	14.68
ChCl-U | 20 wt% H_2O | 10 wt% AC	27.8	27.29
ChCl-U | 30 wt% H_2O | 10 wt% AC	19.3	39.39

higher electric potentials, resulting in increased values and reduced conductivity of the dilute stream due to enhanced salt removal. At 2.2 V, the highest current values were recorded, with the current decreasing proportionally as the applied potential difference decreased. For the ChCl-U flow electrode with 10 wt% H_2O and 10 wt% AC, an electric current of 92 mA was achieved, and the conductivity of the dilute stream measured 0.46 mS/cm (Fig. 5a and b). This represents a 1.12-fold increase in current and nearly a 2-fold reduction in effluent conductivity compared to FCDI desalination with an aqueous flow electrode. However, the pH of the dilute stream, despite being lower than that when using aqueous flow electrodes, remained relatively high at approximately 8.2 (Fig. 6). When employing the DES flow electrode with 20 wt% H_2O content, the current at 2.2 V was slightly lower (87 mA) (Fig. 5a), but the pH of the dilute stream remained stable, making it suitable for drinking purposes (Fig. 6). For the ChCl-U flow electrode with 30 wt% H_2O, the current rose to 94 mA (Fig. 5a), although this was accompanied by a pH increase to 8.6 in the dilute stream (Fig. 6).

The non-monotonic trend in electric current values in FCDI stacks with DES flow electrodes (92 mA with 10 wt% of H_2O, 87 mA with 20 wt % of H_2O, and 94 mA with 30 wt% of H_2O) at 2.2 V can be attributed to the interaction between enhanced ionic mobility and variations in the microstructure of the slurry system. Table 1 shows that adding water to the DES flow electrode decreases its viscosity and increases its conductivity. However, the electrochemical response of the flow electrode system is affected by viscoelastic behaviour, dispersion stability, and the effective percolation of conductive pathways within the flow electrode. Specifically:

- With 10 wt% of water, the system experiences decreased viscosity and a slight increase in conductivity, leading to higher current levels.
- With 20 wt% of water, as conductivity continues to rise, the system exhibits increased elastic (gel-like) properties, as shown in Fig. 9b. This may reduce ion mobility, resulting in a marginally lower current.
- With 30 wt% of water, the lowest viscosity and highest conductivity produce the highest current, but this also causes partial disruption of the DES structure, as indicated by DSC analysis (Fig. 9a), and a

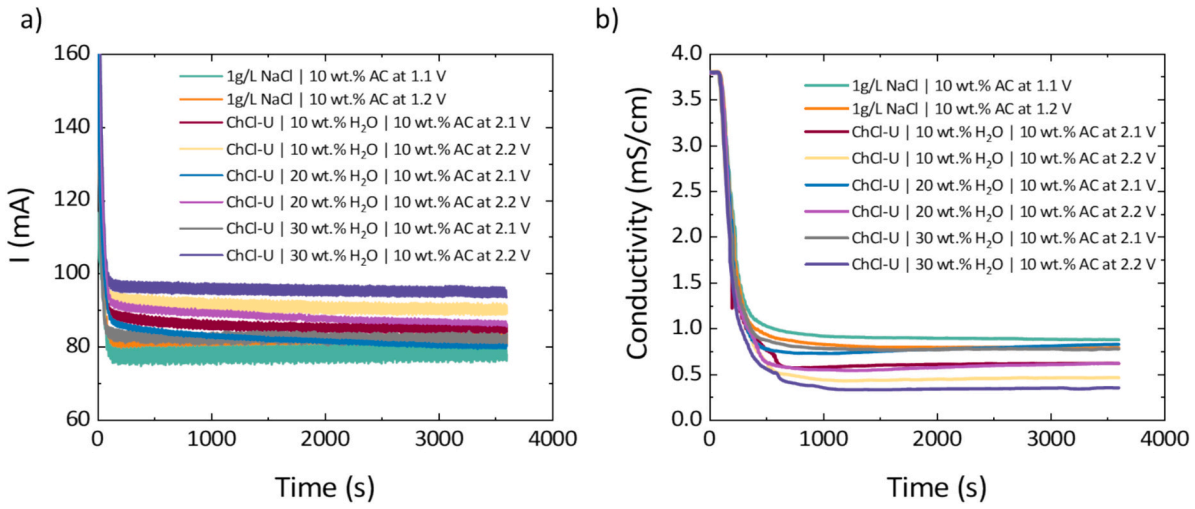

Fig. 5. (a) Chronoamperometric curves and (b) dilute stream conductivity for FCDI stacks using 1 g/L NaCl aqueous flow electrode and different DES flow electrodes during desalination of 1.5 g/L NaCl solution.

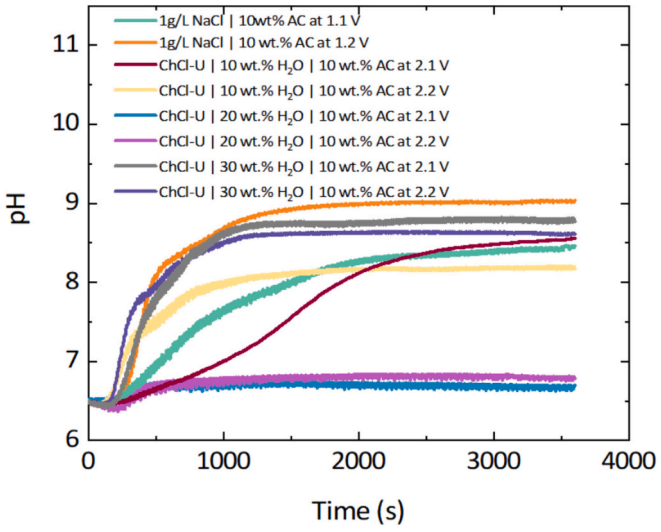

Fig. 6. Dilute stream pH fluctuations when using different flow electrodes in FCDI desalination experiments for the most relevant electric potential differences (all results are shown in Fig. S4).

noticeable increase in the pH of the dilute stream, hinting at the initiation of undesirable electrochemical side reactions.

The desalination efficiency and rate values (Fig. 7a and b) further illustrate that the use of DES flow electrodes, in conjunction with the application of higher voltages, enhances desalination.

The use of a 1 g/L NaCl 10 wt% AC aqueous flow electrode at 1.2 V exhibits a desalination efficiency of 79 %. However, the pH of the dilute stream increased to 9, rendering it unsuitable for potable water use, as previously discussed (Figs. 7a and 6).

The implementation of the ChCl-U flow electrode with 20 wt% H_2O and 10 wt% AC yielded the most favourable results regarding the pH of the obtained effluent, achieving a desalination efficiency of 83 % and a desalination rate of 0.17 mg/cm^2.min at 2.2 V. This results in a more efficient use of charge per unit of salt removed, compared to the use of aqueous flow electrodes, which partially offsets the higher voltage in terms of energy consumption. Increasing the water content to 30 wt% in the flow electrode further improved both the desalination efficiency and rate. Nevertheless, it also caused an undesirable increase in the pH of dilute water (Figs. 7 and 6). In the case of the flow electrode containing 10 wt% H_2O, the desalination efficiency and rate were slightly higher compared to the ChCl-U flow electrode with 20 wt% H_2O and 10 wt% AC. However, as previously observed, the pH of the dilute water did not meet the required quality standards (Figs. 7 and 6). Thus, the

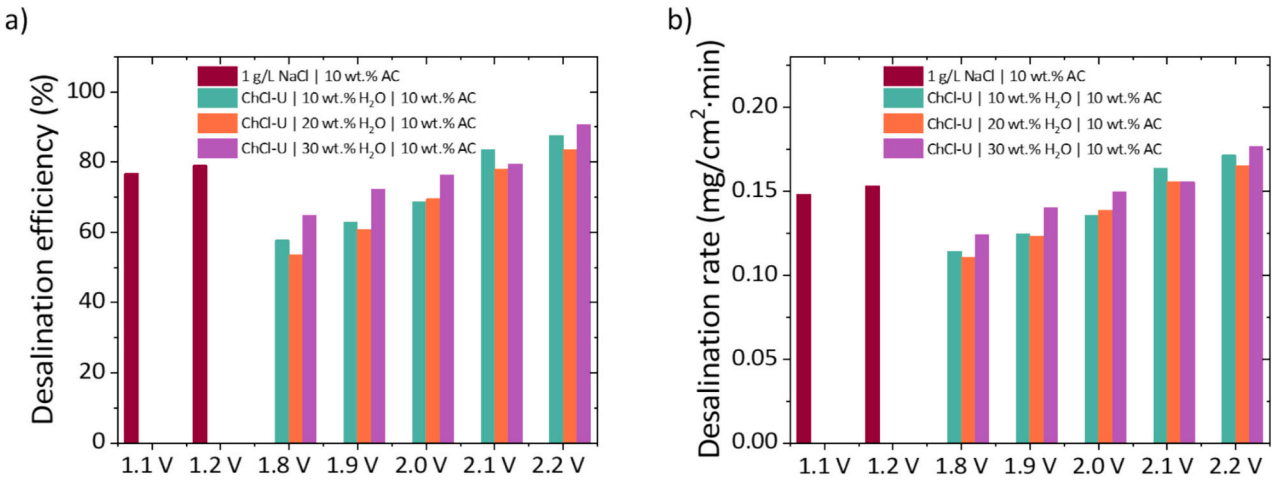

Fig. 7. (a) Desalination efficiency and (b) desalination rate for various flow electrodes during the desalination of a 1.5 g/L NaCl solution.

implication for desalination performance is that higher current does not necessarily lead to better results, especially when considering system stability and effluent quality.

To confirm that the dilute stream did not contain any traces of the deep eutectic solvent, ^{1}H NMR analysis was conducted on the dilute streams obtained when the ChCl-U flow electrode with 20 wt% H_2O and 10 wt% AC was used at 2.1 V and 2.2 V (Fig. 8). The analysis confirmed that no detectable traces of the deep eutectic solvent components, ChCl and U, were present in the dilute stream. This outcome is likely attributable to the stability of the employed DES, reinforced by the design of the desalination cell, which incorporates anion-exchange membranes to separate the flow electrode compartments. These membranes effectively repel choline, a positively charged compound, preventing its migration into dilute streams.

3.3. DSC and viscoelastic properties of DES and aqueous flow electrodes

To better understand the phenomenon underlying the enhanced desalination performance observed when using the DES flow electrode with 20 wt% H_2O, differential scanning calorimetry (DSC) and viscoelastic measurements were conducted (Fig. 9).

DSC analysis revealed that the addition of water significantly reduced the melting temperature of the deep eutectic solvent. ChCl-U exhibited a melting temperature of 16 °C, which decreased to −10 °C upon the doping of 10 wt% H_2O and further dropped to −20 °C with 20 wt% H_2O. These low melting points are significant for the practical application of DES flow electrodes in real environments because they ensure that these flow electrodes remain flowable even at low temperatures. In the case of the ChCl-U flow electrode containing 30 wt% H_2O and 10 wt% AC, the sample no longer exhibited the characteristics of a deep eutectic solvent, indicating an excess of water in the system.

The influence of water on the DES flow electrode was evaluated using viscoelastic measurements, focusing on the elastic (G') and viscous (G'') moduli (Fig. 9b). G' represents the solid-like properties of the flow electrode, whereas G'' corresponds to the liquid-like characteristics, with both parameters derived from sweep oscillatory measurements. The results revealed that both flow electrodes containing 10 and 20 wt% water exhibited predominantly elastic behaviour ($G' > G''$), indicating gel-like structures. Interestingly, the DES flow electrode with 20 wt% water displayed a higher elastic modulus compared to that with 10 wt% water, which was unexpected given the lower viscosity of the electrode with higher water content. This apparent contradiction between lower viscosity and higher elasticity implies a complex interplay between water, the DES matrix, and the dispersed activated carbon particles. It is likely that water not only reduces bulk viscosity by weakening the overall solvent structure but also promotes more effective bridging or clustering of particles through hydrogen bonding or hydration forces, leading to a stronger viscoelastic network under dynamic deformation.

However, this hypothesis requires further investigation. To elucidate the underlying interactions and transitions in the system, a more comprehensive rheological study involving a broader range of water and activated carbon contents is necessary. Although beyond the scope of the present work, such an investigation would provide valuable insights into the design of optimal flow electrode formulations for FCDI applications.

Overall, the aforementioned findings demonstrate and validate the potential of using DES flow electrodes in FCDI.

3.4. Preliminary cost comparison between aqueous and DES flow electrodes

The deep eutectic solvent used in this study, choline chloride–urea (ChCl–U), consists of two inexpensive and widely available components. Based on industrial bulk prices, choline chloride costs around €3.00 per kilogram, and urea costs about €0.50 per kilogram. With a molar ratio of 1:2 (ChCl:Urea), the resulting ChCl–U DES has an estimated cost of €1.80 to €2.00 per kilogram when purchased in bulk. In the optimised electrolyte formulation employed here, an extra 20 wt% water is added, lowering the cost to roughly €1.60 per kilogram of the final electrolyte

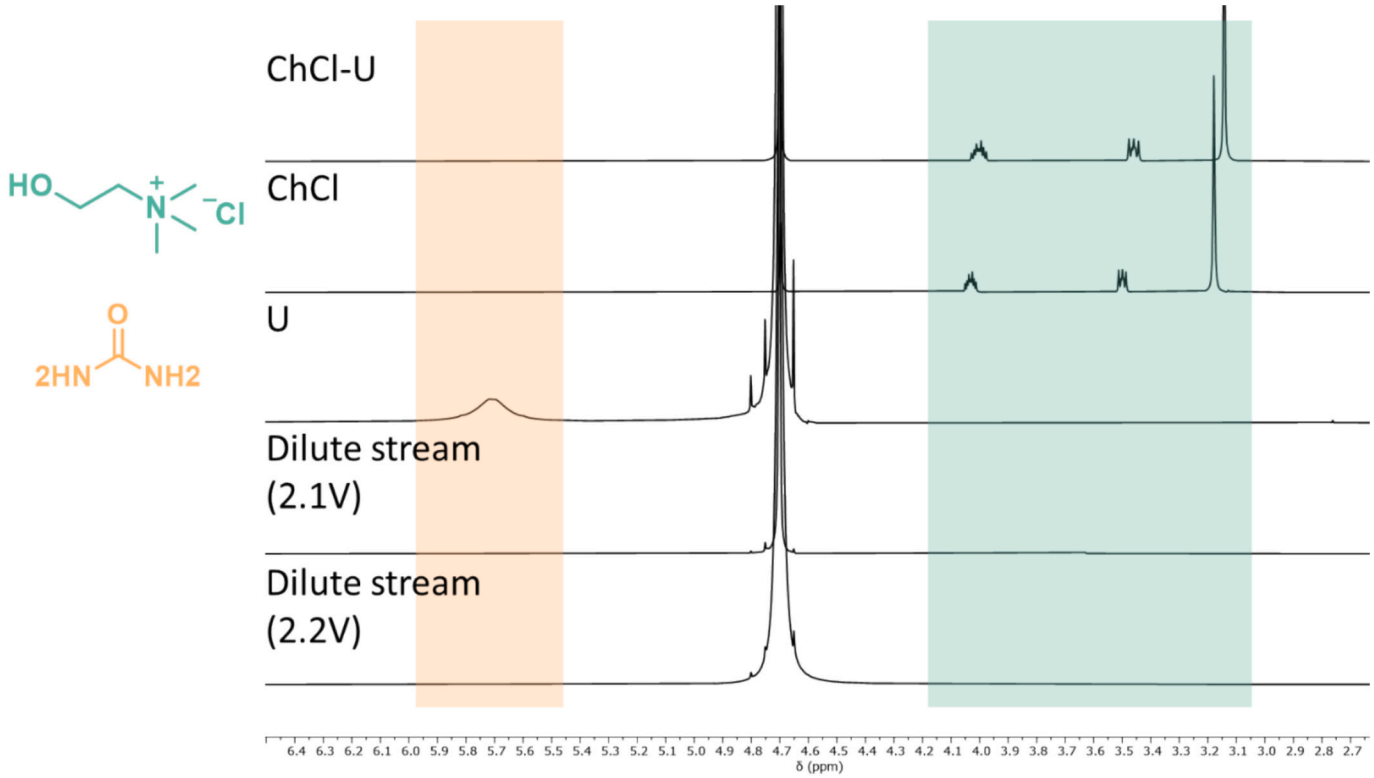

Fig. 8. ^{1}H NMR analysis of the dilute steam when 2.1 V and 2.2 V were applied and their comparison with the spectra of the starting compounds (ChCl and U) and the deep eutectic solvent (ChCl-U).

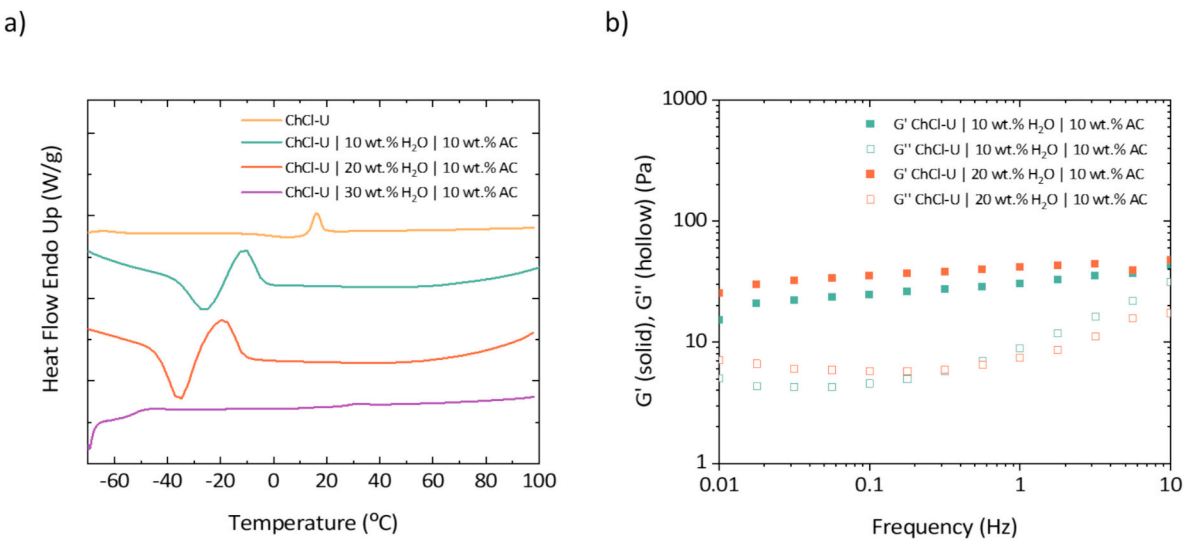

Fig. 9. (a) DSC and (b) viscoelastic properties of the DES flow electrodes.

mixture. Although this is higher than the cost of a traditional aqueous electrolyte (e.g., 1 g/L NaCl solution, <€0.10 per kg), electrolyte expenses are only a small part of the overall costs in FCDI processes. Furthermore, the wider electrochemical stability window of ChCl–U (up to 2.2 V) enables higher desalination efficiency and, for instance, may help reduce the membrane area and equipment costs, potentially compensating for the somewhat higher electrolyte price. Additionally, preparing ChCl–U involves simple mixing and heating steps (70 °C), without the need for complex synthesis or purification, which keeps processing costs low and enables scalability. Furthermore, unlike water, the employed DES did not migrate through membranes and is non-volatile at room temperature, enabling the maintenance of a constant flow electrode composition in a closed cycle. These factors together highlight the practical feasibility and potential cost competitiveness of DES flow electrodes for FCDI applications.

4. Conclusions

This study introduced for the first time the use of deep eutectic solvents (DES) as flow electrodes in flow electrode capacitive deionisation (FCDI) systems for desalination applications. By utilising ChCl-U, which possesses a broader electrochemical stability window than water, the applied voltage was increased beyond 1.2 V without inducing electrolysis, thereby enhancing desalination rates.

The doping of water into the ChCl-U reduced its viscosity, enabling its application in FCDI flow electrodes while maintaining electrochemical stability. Among the compositions studied, the ChCl-U flow electrode containing 20 wt% water and 10 wt% activated carbon achieved the optimal balance of desalination efficiency (83 %), rate (0.17 mg/cm^2·min), and effluent quality, underscoring it as a viable alternative to aqueous flow electrodes. However, long-term operational assessments are still necessary to fully understand the long-term impact of DES flow electrodes on the stability of ion-exchange membranes and flow electrode materials as part of future optimisation and scale-up studies. Overall, this study highlights the transformative potential of DES flow electrodes to enhance the performance of desalination processes. By facilitating higher operational voltages and improved efficiency, DES flow electrodes present a promising pathway for the development of more efficient FCDI desalination technologies.

Declaration of competing interest

The authors declare that they have no known competing financial interests or personal relationships that could have appeared to influence the work reported in this paper.

Acknowledgments

Elena Gabirondo acknowledges the Basque Government for her postdoctoral fellowship POS_2022_1_0040 and Hafiz M. Saif is grateful to *Fundação para a Ciência e Tecnologia* (FCT/MCTES) for his PhD grant 2020.09828.BD (doi:10.54499/2020.09828.BD). This work received funding from the FCT/MCTES under grant agreement No PTDC/EQU-EQU/6193/2020 (Se(*L*)ect(i)vity) and LISBOA2030-FEDER-00729800 (n° 16144 – Li-cycle). This work was also supported by the following research centres financed by national Portuguese funds from FCT/MCTES: Associate Laboratory for Green Chemistry – LAQV (UIDB/50006/2023), LEAF (UIDB/04129/2020), CEMMPRE (UID/EMS/00285/2020) and ARISE (LA/P/0112/2020).

Appendix A. Supplementary data

Supplementary data to this article can be found online at https://doi.org/10.1016/j.desal.2025.119218.

Data availability

Data will be made available on request.

References

[1] European Courts of Auditors, Sustainable Water Use in Agriculture: CAP Funds More Likely to Promote Greater Rather Than More Efficient Water Use, 2021 (Luxembourg).
[2] C.J. Vörösmarty, P.B. McIntyre, M.O. Gessner, D. Dudgeon, A. Prusevich, P. Green, S. Glidden, S.E. Bunn, C.A. Sullivan, C.R. Liermann, P.M. Davies, Global threats to human water security and river biodiversity, Nat 467 (2010) 555–561, https://doi.org/10.1038/nature09440.
[3] P.H. Gleick, Global freshwater resources: soft-path solutions for the 21st century, Science 302 (2003) 1524–1528, https://doi.org/10.1126/SCIENCE.1089967.
[4] S. Pawlowski, R.M. Huertas, C.F. Galinha, J.G. Crespo, S. Velizarov, On operation of reverse electrodialysis (RED) and membrane capacitive deionisation (MCDI) with natural saline streams: a critical review, Desalination 476 (2020) 114183, https://doi.org/10.1016/J.DESAL.2019.114183.
[5] C. Zhang, J. Ma, L. Wu, J. Sun, L. Wang, T. Li, T.D. Waite, Flow electrode capacitive deionization (FCDI): recent developments, environmental applications, and future perspectives, Environ. Sci. Technol. 55 (2021) 4243–4267, https://doi.org/10.1021/ACS.EST.0C06552.
[6] H.M. Saif, J.G. Crespo, S. Pawlowski, Lithium recovery from brines by lithium membrane flow capacitive deionization (Li-MFCDI) – a proof of concept, J. Membr. Sci. Lett. 3 (2023) 100059, https://doi.org/10.1016/j.memlet.2023.100059.

[7] M.M. AL-Rajabi, F.A. Abumadi, T. Laoui, M.A. Atieh, K.A. Khalil, Capacitive deionization for water desalination: cost analysis, recent advances, and process optimization, J Water Process Eng 58 (2024) 104816, https://doi.org/10.1016/J.JWPE.2024.104816.

[8] N.A.T. Tran, N.M. Phuoc, T.M. Khoi, H. Bin Jung, N. Cho, Y.W. Lee, E. Jung, B. G. Kang, K. Park, J. Hong, C.Y. Yoo, H.S. Kang, Y. Cho, Electroactive self-polymerized dopamine with improved desalination performance for flow- and fixed-electrodes capacitive deionization, Appl. Surf. Sci. 579 (2022) 152154, https://doi.org/10.1016/J.APSUSC.2021.152154.

[9] A. Hassanvand, G.Q. Chen, P.A. Webley, S.E. Kentish, An investigation of the impact of fouling agents in capacitive and membrane capacitive deionisation, Desalination 457 (2019) 96–102, https://doi.org/10.1016/J.DESAL.2019.01.031.

[10] Y.U. Shin, J. Lim, C. Boo, S. Hong, Improving the feasibility and applicability of flow-electrode capacitive deionization (FCDI): review of process optimization and energy efficiency, Desalination 502 (2021) 114930, https://doi.org/10.1016/J.DESAL.2021.114930.

[11] J. Ma, C. Zhai, F. Yu, Review of flow electrode capacitive deionization technology: research progress and future challenges, Desalination 564 (2023) 116701, https://doi.org/10.1016/J.DESAL.2023.116701.

[12] J. Ma, L. Chen, F. Yu, Environmental applications and perspectives of flow electrode capacitive deionization (FCDI), Sep. Purif. Technol. 335 (2024) 126095, https://doi.org/10.1016/J.SEPPUR.2023.126095.

[13] J. Ma, J. Ma, C. Zhang, J. Song, W. Dong, T.D. Waite, Flow-electrode capacitive deionization (FCDI) scale-up using a membrane stack configuration, Water Res. 168 (2020) 115186, https://doi.org/10.1016/J.WATRES.2019.115186.

[14] R. Chen, X. Liu, M. Wang, Y. Shu, M. Zhang, B. Liu, Z. Wang, A novel two-stage continuous capacitive deionization system with connected flow electrode and freestanding electrode, Chem. Eng. J. 491 (2024) 152133, https://doi.org/10.1016/J.CEJ.2024.152133.

[15] H.M. Saif, J.G. Crespo, S. Pawlowski, Can 3D-printed flow electrode gaskets replace CNC-milled graphite current collectors in flow capacitive deionization? Desalination 597 (2025) 118362 https://doi.org/10.1016/j.desal.2024.118362.

[16] G. Folaranmi, M. Tauk, M. Bechelany, P. Sistat, M. Cretin, F. Zaviska, Investigation of fine activated carbon as a viable flow electrode in capacitive deionization, Desalination 525 (2022) 115500, https://doi.org/10.1016/J.DESAL.2021.115500.

[17] M. Tauk, G. Folaranmi, M. Cretin, M. Bechelany, P. Sistat, C. Zhang, F. Zaviska, Recent advances in capacitive deionization: a comprehensive review on electrode materials, J. Environ. Chem. Eng. 11 (2023) 111368, https://doi.org/10.1016/J.JECE.2023.111368.

[18] W. Zhang, W. Xue, K. Xiao, C. Visvanathan, J. Tang, L. Li, Selection and optimization of carbon-based electrode materials for flow-electrode capacitive deionization, Sep. Purif. Technol. 315 (2023) 123649, https://doi.org/10.1016/J.SEPPUR.2023.123649.

[19] I.A. Kinloch, J. Suhr, J. Lou, R.J. Young, P.M. Ajayan, Composites with carbon nanotubes and graphene: an outlook, Science 362 (2018) 547–553, https://doi.org/10.1126/science.10899.

[20] G. Kothandam, G. Singh, X. Guan, J.M. Lee, K. Ramadass, S. Joseph, M. Benzigar, A. Karakoti, J. Yi, P. Kumar, A. Vinu, Recent advances in carbon-based electrodes for energy storage and conversion, Adv. Sci. 10 (2023) 2301045, https://doi.org/10.1002/ADVS.202301045.

[21] Y. Liu, L. Wang, Q. Ma, X. Xu, X. Gao, H. Zhu, T. Feng, X. Dou, M. Eguchi, Y. Yamauchi, X. Yuan, Simultaneous generation of residue-free reactive oxygen species and bacteria capture for efficient electrochemical water disinfection, Nat. Commun. 15 (2024) 10175, https://doi.org/10.1038/s41467-024-53174-9.

[22] Z. Guo, G. Shen, Z. Wang, Q. Ma, L. Zhang, B. Xiao, Y. Yan, Y. Zheng, Y. Liu, X. Yuan, Integrating FeOOH with bacterial cellulose-derived 3D carbon nanofiber aerogels for fast and stable capacitive deionization based on accelerating chloride insertion, Desalination 576 (2024) 117329, https://doi.org/10.1016/J.DESAL.2024.117329.

[23] Q. Ma, Z. Wang, L. Zhang, B. Xiao, L. Zhang, C. Xiao, W. Zhang, J. Xia, Y. Liu, X. Yuan, Marrying Fe nanoclusters with 3D carbon nanofiber aerogels: triggering fast and robust faradic capacitive deionization, Sep. Purif. Technol. 353 (2025) 128503, https://doi.org/10.1016/J.SEPPUR.2024.128503.

[24] B. Xiao, L. Zhang, Q. Ma, Z. Hua, X. Luan, J. Xia, W. Zhang, Z. Zuo, X. Yuan, Y. Liu, Bacterial cellulose: a versatile 3D nanostructure advancing electrode engineering for high-performance capacitive deionization, Desalination 612 (2025) 118955, https://doi.org/10.1016/J.DESAL.2025.118955.

[25] Y. Cho, C.Y. Yoo, S.W. Lee, H. Yoon, K.S. Lee, S.C. Yang, D.K. Kim, Flow-electrode capacitive deionization with highly enhanced salt removal performance utilizing high-aspect ratio functionalized carbon nanotubes, Water Res. 151 (2019) 252–259, https://doi.org/10.1016/J.WATRES.2018.11.080.

[26] H. Wang, W. Sun, Y. Liu, H. Ma, T. Li, K.A. Lin, K. Yin, S. Luo, Large-scale chemical vapor deposition synthesis of graphene nanoribbions/carbon nanotubes composite for enhanced membrane capacitive deionization, J. Electroanal. Chem. 904 (2022) 115907, https://doi.org/10.1016/J.JELECHEM.2021.115907.

[27] Z. Wang, Y. Hu, Q. Wei, W. Li, X. Liu, F. Chen, Enhanced desalination performance of a flow-electrode capacitive deionization system by adding vanadium redox couples and carbon nanotubes, J. Phys. Chem. C 125 (2021) 1234–1239, https://doi.org/10.1021/ACS.JPCC.0C09058.

[28] F.A. AlMarzooqi, A.A. Al Ghaferi, I. Saadat, N. Hilal, Application of capacitive deionisation in water desalination: a review, Desalination 342 (2014) 3–15, https://doi.org/10.1016/J.DESAL.2014.02.031.

[29] B.B. Hansen, S. Spittle, B. Chen, D. Poe, Y. Zhang, J.M. Klein, A. Horton, L. Adhikari, T. Zelovich, B.W. Doherty, B. Gurkan, E.J. Maginn, A. Ragauskas, M. Dadmun, T.A. Zawodzinski, G.A. Baker, M.E. Tuckerman, R.F. Savinell, J. R. Sangoro, Deep eutectic solvents: a review of fundamentals and applications, Chem. Rev. 121 (2021) 1232–1285, https://doi.org/10.1021/ACS.CHEMREV.0C00385.

[30] A. Prabhune, R. Dey, Green and sustainable solvents of the future: deep eutectic solvents, J. Mol. Liq. 379 (2023) 121676, https://doi.org/10.1016/J.MOLLIQ.2023.121676.

[31] P.A. Mercadal, A. González, A. Beloqui, L.C. Tomé, D. Mecerreyes, M. Calderón, M. L. Picchio, Eutectogels: the multifaceted soft ionic materials of tomorrow, JACS Au 4 (2024) 3744–3758, https://doi.org/10.1021/JACSAU.4C00677.

[32] L.C. Tomé, D. Mecerreyes, Emerging ionic soft materials based on deep eutectic solvents, J. Phys. Chem. B 124 (2020) 8465–8478, https://doi.org/10.1021/ACS.JPCB.0C04769.

[33] Z. Jie Zhang, X. Ying Chen, H. Jie Feng, High-voltage and wide temperature aqueous supercapacitors aided by deep eutectic solvents, J. Electroanal. Chem. 908 (2022) 116082, https://doi.org/10.1016/J.JELECHEM.2022.116082.

[34] Q. Li, J. Jiang, G. Li, W. Zhao, X. Zhao, T. Mu, The electrochemical stability of ionic liquids and deep eutectic solvents, Sci. China Chem. 59 (2016) 571–577, https://doi.org/10.1007/S11426-016-5566-3.

[35] D. Julião, M. Xavier, X. Mascarenhas, Deep eutectic solvents: viable sustainable electrolytes for supercapacitors, Mater. Today Energy 42 (2024) 101432, https://doi.org/10.1016/J.MTENER.2023.101432.

[36] S. Azmi, M.F. Koudahi, E. Frackowiak, Reline deep eutectic solvent as a green electrolyte for electrochemical energy storage applications, Energy Environ. Sci. 15 (2022) 1156–1171, https://doi.org/10.1039/D1EE02920G.

[37] H.M. Saif, B. Ferrández-Gómez, V.D. Alves, R.M. Huertas, G. Alemany-Molina, A. Viegas, E. Morallón, D. Cazorla-Amorós, J.G. Crespo, S. Pawlowski, Activated carbons for flow electrode capacitive deionization (FCDI) – morphological, electrochemical and rheological analysis, Desalination 602 (2025) 118638, https://doi.org/10.1016/J.DESAL.2025.118638.

[38] R.F.W.J.S. Petek, J. Tyler, Nathaniel C. Hoyt, T.J. Savinell, N.C. Petek, R.F. Hoyt, J. S. Savinell, Wainright, Characterizing slurry electrodes using electrochemical impedance spectroscopyle, J. Electrochem. Soc. 163 (2016) A5001, https://doi.org/10.1149/2.0011601JES.

[39] H.M. Saif, J.G. Crespo, S. Pawlowski, How should flow electrode capacitive deionization (FCDI) be operated to achieve efficient desalination and scalability? Desalination 606 (2025) 118769 https://doi.org/10.1016/J.DESAL.2025.118769.

[40] H.M. Saif, T.H. Gebregeorgis, J.G. Crespo, S. Pawlowski, The influence of flow electrode channel design on flow capacitive deionization performance: experimental and CFD modelling insights, Desalination 578 (2024) 117452, https://doi.org/10.1016/J.DESAL.2024.117452.

[41] M. Li, C. Zhu, T. Fu, X. Gao, Y. Ma, Effect of water on amine-based deep eutectic solvents (choline chloride + monoethanolamine): structure and physicochemical properties, J. Environ. Chem. Eng. 10 (2022) 106952, https://doi.org/10.1016/J.JECE.2021.106952.

[42] S. Rozas, C. Benito, R. Alcalde, M. Atilhan, S. Aparicio, Insights on the water effect on deep eutectic solvents properties and structuring: the archetypical case of choline chloride + ethylene glycol, J. Mol. Liq. 344 (2021) 117717, https://doi.org/10.1016/J.MOLLIQ.2021.117717.

[43] D. He, C.E. Wong, W. Tang, P. Kovalsky, T. David Waite, Faradaic reactions in water desalination by batch-mode capacitive deionization, Environ. Sci. Technol. Lett. 3 (2016) 222–226, https://doi.org/10.1021/ACS.ESTLETT.6B00124.

[44] J.E. Dykstra, K.J. Keesman, P.M. Biesheuvel, A. van der Wal, Theory of pH changes in water desalination by capacitive deionization, Water Res. 119 (2017) 178–186, https://doi.org/10.1016/J.WATRES.2017.04.039.